RECENT

An Implementation of the Radon Transformation for Features Estimation of Image-Objects with Symmetry

Adrian DANILA

Transilvania University of Brasov, Romania, adrian.danila@unitbv.ro

Abstract

In this paper we develop a method for estimating the direction of symmetry and the mass-centre coordinates of the image objects with symmetry. The proposed method is based on the estimation of the axes of symmetry of the image-object by means of its enclosing equivalent ellipse. The coordinates of the mass-centre and the directions of the main axes of the equivalent ellipse are estimated with the Radon transformation method. Within the paper we propose the implementation of a forgetting-factor-type 2D filter that improves the accuracy of the estimate, especially for the blurred and noisy images.

Keywords

image analysis, Radon transformation, direction estimation, digital image processing

1. Introduction

Estimating the spatial coordinates and trajectory based on the analysis of the images taken from the scene is a common problem in many applications such as: in robotics - obstacles avoidance and autonomous routing - [2, 3], in pattern recognition, in the detection of aircraft by radar, [1] as well as in many other areas. In the literature, constant attention has been paid to the mentioned issues which led to the development of sophisticated solving techniques based on numerous analytical or heuristic principles, [5, 6, 7].

A case commonly encountered in practice is the estimation of the centre and the direction of the axis of symmetry for the graphical objects that feature one axis of symmetry. Figure 1 shows four examples of this category. Numerous other examples may be added: graphic signs indicating directions, airplanes and ships, the texture on the surface of bodies, etc.

| (a) | (b) | (c) | (d) |
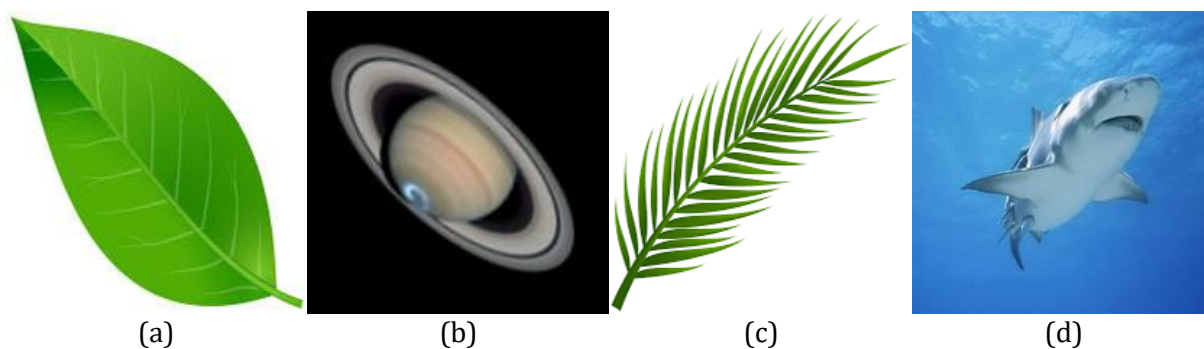
Fig. 1. Examples of image-objects with axial symmetry. (a)- continuous margins; (b)- continuous margins, gaps within the domain of image; (c)- discontinuous margins; (d)- discontinuous margins and blur

The Radon transformation's basic field of implementation is the medical tomography for the reconstruction of the three-dimensional images based on Roentgen projections. Another implementation of the Radon transformation is the identification of lines. Image Processing and the Computer Vision science benefit of this approach. The method is accurate and robust to the scene's noises.

There have also been developed algorithms that allow identification of second-order curves - ellipses, parabolas, etc. -, but the implementation of these algorithms is not straightforward [4, 9].

2. Objectives and Approach

The principle of identifying straight lines in the field of a 2D-image is based on the identification of the coordinates at the points of the maxima in the plane of the Radon transformation, [4]. In this paper we propose to use the Radon transformation method for estimating the coordinates of the centre of symmetry and the directions of the main axes of symmetry for images-objects with symmetry, as shown in Figure 1.

The basic idea of this work is to estimate the axis of symmetry of a given image-object, within a 2D-image by means of its equivalent enclosing ellipse. The reason of this approach is that the ellipse is the 2D closed-curve with the least number of parameters that conserves both symmetry and orientation.

The estimations are made as follows:

(a) The main axis of the ellipse and the angle between the major axis of the ellipse and the vertical axis of the reference coordinate system are estimated by means of the evaluation of the Radon transform i.e. the projections of the image-object.

(b) The absolute maximum and the minimum values of the Radon transform with respect to the projection angle provide information about the angle between the axes of the equivalent ellipse and the axes of the reference coordinate system.

(c) The relative maximum of the projections at the directions of the reference coordinate system provide information about the centre of the equivalent ellipse.

3. Methods

The Radon transformation in the field of the continuous 2D space is well documented in the literature, [1-4, 7, 9]. For the case of infinitely expanded 2D-plane, the Radon's transform of a function, $f(x; y)$ on the direction of a line, (d) is given by the following line-integral:

$$\{\Re f\}(d,\theta) = \Re\{f(\circ)\} = \int_{(d)} f \, dl \, . \tag{1}$$

Onto the 2D-plane referred to an orthogonal coordinate system, the equation of the line (d) may be written as follows:

$$(d): \quad x\cdot\cos\theta + y\cdot\sin\theta - \zeta = 0 \, . \tag{2}$$

The angle $\theta = \pi/2 - \varphi$, is the angle of inclination of the projection plane - perpendicular to the direction of the line (d) - and (ζ) is the intersection of the line (d) with the vertical axis of the coordinate system.

In this case, the Radon transform in expression (1) for an arbitrary function $f(x; y)$ transforms to a double integral as follows [9]:

$$\Re\{f(x,y);\theta,\zeta\} = \int_{-\infty}^{+\infty}\int_{-\infty}^{+\infty} f(x,y)\cdot\delta(x\cdot\cos\theta + y\cdot\sin\theta - \zeta)\,dxdy \, , \tag{3}$$

where δ represents the unit-impulse function. The function $f(x; y)$ represents the intensity of the image at the specified coordinates point, $(x; y)$ [1, 6].

In the followings we consider the model depicted in Figure 2 and we compute the expression of the Radon transform.
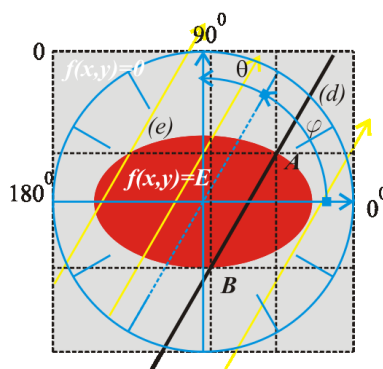
Fig. 2. The model for estimating the geometric parameters of an ellipse by means of the Radon transformation

The equations of the ellipse – (*e*), the straight-line – (*d*) and the expression of the function $f(x; y)$ are as follows:

$$(d): \quad x \cdot \cos\theta + y \cdot \sin\theta - \zeta = 0; \quad (e): \quad \frac{x^2}{\alpha^2} + \frac{y^2}{\beta^2} - 1 = 0; \tag{4}$$

$$f(x, y) = \begin{cases} E & (x, y) \in Int(e) \\ 0 & (x, y) \in \Re \times \Re - Int(e) \end{cases}. \tag{5}$$

In the expressions above, α, β are the major and the minor axes and, $Int(e)$ is the interior of the ellipse (*e*), respectively.

We rewrite the expression of (*d*) in parametric form and compute the expression of the Radon transform of $f(x; y)$ onto the path (*d*):

$$\begin{cases} x = t \\ y = \dfrac{1}{\sin\varphi} \cdot (-t \cdot \cos\theta + \zeta) \end{cases}; \Rightarrow \begin{cases} x' = 1 \\ y' = \dfrac{-\cos\theta}{\sin\theta} \end{cases}; \Rightarrow \sqrt{x'^2 + y'^2} = \frac{1}{\sin\theta} \Rightarrow dl = \frac{dt}{\sin\theta}; \tag{6}$$

$$\Re\{f; \theta, \zeta\} = \int_{(d)} f \, dl = \int_{x_B}^{x_A} E \cdot \frac{1}{\sin\theta} dt = \frac{E}{\sin\theta} \cdot (x_A - x_B).$$

The values of the abscissas x_A; x_B of the intersection points *A*; *B* may be computed from the equations set (4):

$$x_{A,B} = \frac{\alpha^2 \cdot \zeta \cdot \cos\theta \pm \alpha \cdot \beta \cdot \sin\theta \cdot \sqrt{-\zeta^2 + \beta^2 \cdot \sin^2\theta + \alpha^2 \cdot \cos^2\theta}}{\beta^2 \cdot \sin^2\theta + \alpha^2 \cdot \cos^2\theta}. \tag{7}$$

From the expressions (6) and (7), follows:

$$\Re\{f; \theta, \zeta\} = 2 \cdot E \cdot \alpha \cdot \beta \cdot \sin\theta \cdot \frac{\sqrt{-\zeta^2 + \beta^2 \cdot \sin^2\theta + \alpha^2 \cdot \cos^2\theta}}{(\beta^2 \cdot \sin^2\theta + \alpha^2 \cdot \cos^2\theta)}. \tag{8}$$

Three special cases are of interest.
1. Case of the vertical line through the origin: θ = 0; ζ = 0.

$$\Re\{f; 0, 0\} = \Re_{=}\{f\} = 2 \cdot E \cdot \beta. \tag{9}$$

2. Case of the horizontal line through the origin: θ = π/2; ζ = 0.

$$\Re\{f; \pi/2, 0\} = \Re_{\perp}\{f\} = 2 \cdot E \cdot \alpha. \tag{10}$$

3. Case of the horizontal line through the origin: ζ = 0.

$$\Re\{f; \theta, 0\} = \frac{2 \cdot E \cdot \alpha \cdot \beta}{\sqrt{\beta^2 \cdot \sin^2\theta + \alpha^2 \cdot \cos^2\theta}}. \tag{11}$$

From the expressions above one may remark the followings:
1. The ratio $\Re_{\perp}\{f\}/\Re_{=}\{f\} = \alpha/\beta$ only depends on the ratio between the major over minor axes of the ellipse;
2. The term $\beta \le \sqrt{\beta^2 \cdot \sin^2\theta + \alpha^2 \cdot \cos^2\theta} \le \alpha$ represents the distance from the current point onto the ellipse to the origin; Follows that $\Re_{=}\{f\} \le \Re\{f; \theta, 0\} \le \Re_{\perp}\{f\}$;
3. Consider the given parameters α, β and the projection's direction θ is constant. Then, the maximum value of the Radon transform is obtained onto the line that passes through the centre of the ellipse.

For a given fixed ellipse, the function $\Re\{f; \theta, 0\}$ is a function of θ only, thus one may rewrite this function as follows:

$$R_{max}(\theta) = \Re\{f; \theta, 0\}. \tag{12}$$

The functions $\Re\{f; 0, \zeta\}$, $\Re\{f; \pi/2, \zeta\}$ and $R_{max}(\theta)$ are depicted in the left side of Figure 3. Based on the corresponding properties of the Radon transformation, these results apply for the shifted and the rotated ellipse.

The function $R_{max}(\theta)$ is ellipse-translation invariant. If the ellipse is rotated by the initial angle θ_0, then $R_{max}(\theta) = R_{max,0}(\theta + \theta_0)$ shifts by θ_0 with respect to the horizontal aligned ellipse, Figure 3 – right side.
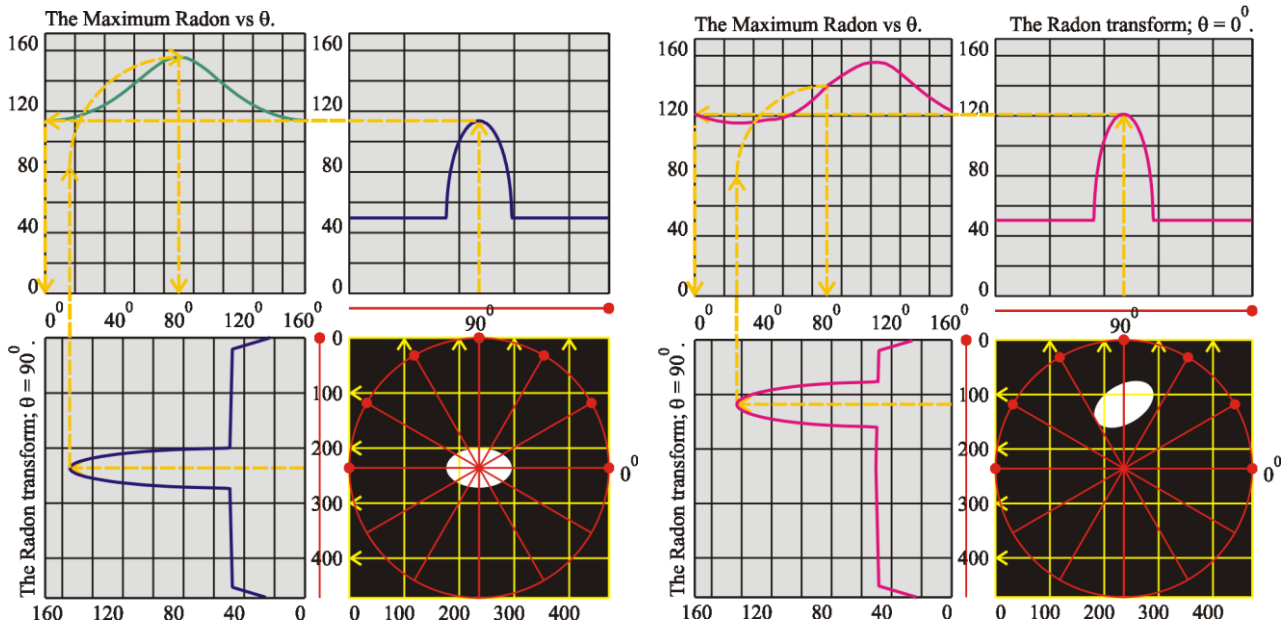
Fig. 3. The Radon Transforms and the maximum Radon function.
To the left - a centred, horizontal aligned ellipse. To the right - a translated and rotated ellipse

In the discretized infinitely expanded space-domain, the double integral transforms into double sums that approximate the transformation's values in the continuous domain. For the finite-meshed space-domains, the calculation of the discrete Radon transform is exact only on the directions of the pixels' rows and columns, i.e. the axis of the image. For the estimation of the discrete Radon transform values on an arbitrary direction – different from the image's axis, interpolations must be made.

This makes the discrete Radon transform on the finite domain to only approximate the discrete Radon transform true values. The rule is: the farther from the centre of image the point is, the less accurate the estimation of the discrete Radon transform.

To eliminate this effect, we propose the use of a method issued from Systems Identification. The degree of correlation of the time- series samples decreases with the degree of anteriority of samples. In the case of time-series with highly correlated samples, the anteriority can be simulated by weighting their amplitude with a subunit factor that decreases with anteriority. This factor is called the forgetting factor [8].

In the case of the 2D images one may observe that the higher the distance between the projection plane and the source, the smaller the contribution of the source to the overall intensity of the projection. Thus, the source intensity can be weighted according to the distance between the centre of the image and the position of the source, to decrease the spatial correlations between them:

$$y[k1;k2] = \lambda^{-OP(k1;k2)} \cdot v[k1;k2], \quad \text{where } k1, k2 \in [N;1]; \lambda \in (0;1]. \tag{13}$$

In (13), $OP(k1;k2)$ represents the Euclidean distance from the centre of the object to the coordinates' point $(k1;k2)$. The intensity of sources at points in the periphery of the image is weighted to zero, which is equivalent to the infinite location of those sources.

For the computer experiments we made and used several dedicated software applications written in the Python ecosystem [4].

We focused on the method's robustness to image's gaps, discontinuities at margins, and blur. The implementation of the proposed 2D forgetting-factor-type filter and the increase of the estimation accuracy were also investigated.

The steps of the experiment were:
1. A greyscale transformation of image.
2. An image threshold.
3. The computations of the Radon transforms on X and Y axes.
4. The estimations of the mass-centre coordinates and the orientation of the main axis.

4. Results and Discussions

The computer experiments were implemented on the images depicted in Figures 1 (a) – (d). In the first and the second steps of the experiments, the grayscale transformation – Figures 4 (a) – (d), and the image threshold - Figures 5 (a) – (d), were implemented.

| (a) | (b) | (c) | (d) |
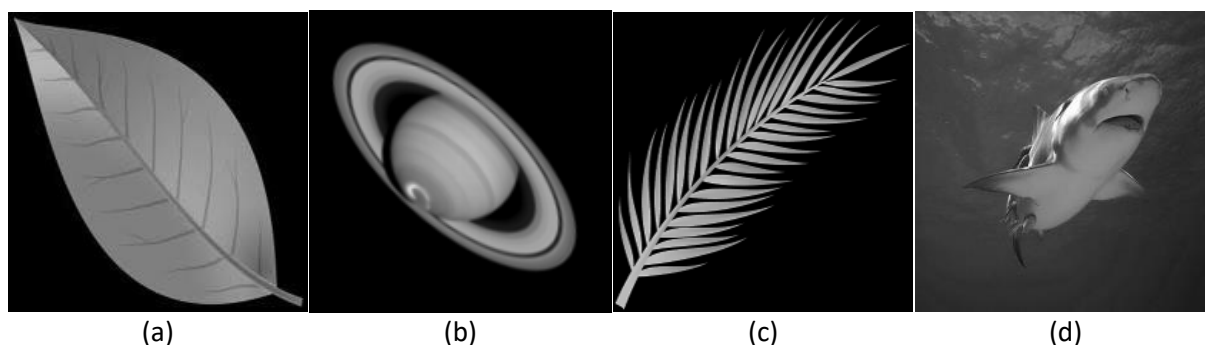
Fig. 4. Images in Figures 1 after the greyscale transformation

| (a) | (b) | (c) | (d) |
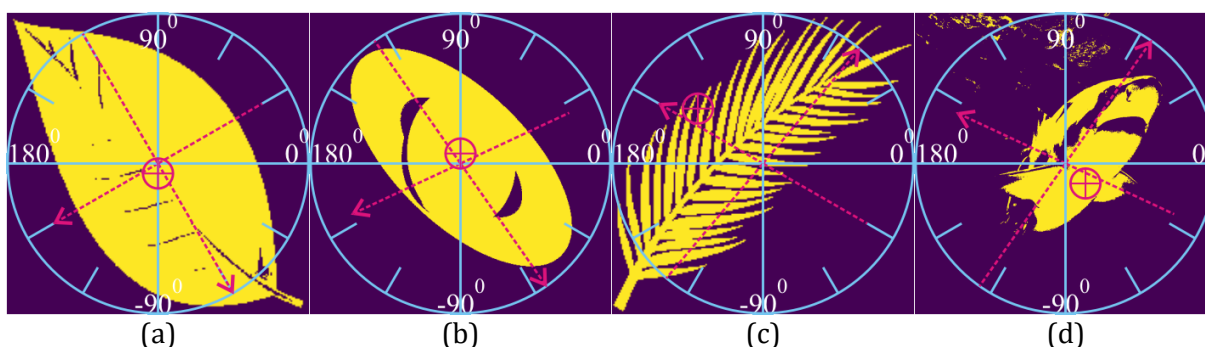
Fig. 5. Threshold, mass-centre and symmetry detection. Images in Figure 4 without filter

Then, the Radon transformations on both X and Y axes were implemented. The resulting samples are of the form of stochastic variables, Figures 6 (a) - (d). The noise amplitude is higher if the image margins are discontinuous, Figure 6 (c), or if blurred image, Figure 6 (d).

| (a) | (b) | (c) | (d) |
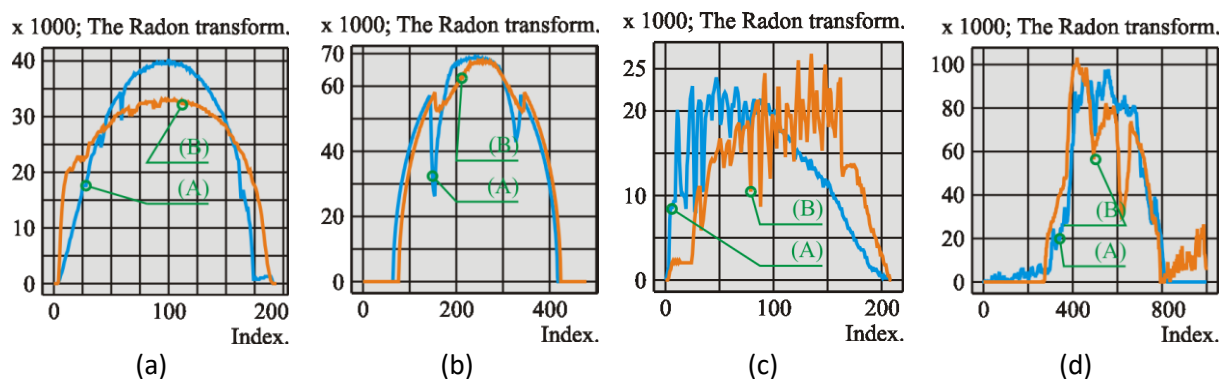
Fig. 6. Estimations for the images in Figures 5.
Plots (A): The Radon transforms on the X-axis. Plots (B): The Radon transforms on the Y-axis

For the not filtered images, the accuracy of the mass-centre estimation is affected by the corrupting noise due to the gaps, margin discontinuities and blur.

The directions of the axis of symmetry are well estimate, Table 1. This remark is true even for the noisy images in Figures 5 (c) and 5 (d).

Table 1. Not filtered images. Estimations of the geometrical parameters

Figure / Image label	Figure 5	(a)	(b)	(c)	(d)
Coordinates of the mass centre	X_0	100	239	47	560
	Y_0	94	257	135	419
Angle of major axis	θ	-60	-55	50	55
Angle between major and minor axis	γ	-90	-100	95	100
Ratio between major and minor axis length	β/α	0.595	0.513	0.354	0.624
Image size	N/N	195/195	480/480	210/210	1000/1000

Figures 7 (a) – (d) depict the estimations made onto the images filtered with the forgetting-factor-type filter with the parameter λ = 0.995.

(a) (b) (c) (d)
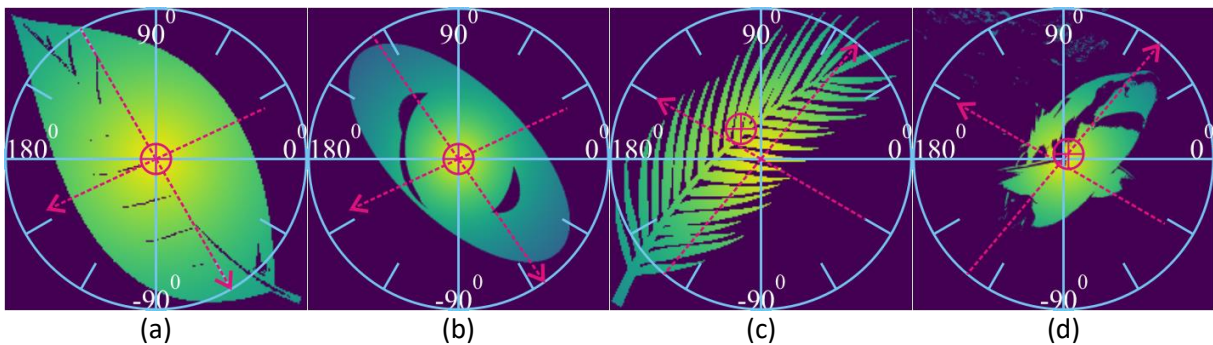
Fig. 7. Threshold, mass-centre and symmetry detection; images in Figure 4 with filter

The Radon transformations on X and Y axes, for the filtered images, are depicted in Figure 8. In comparison with the results in Figure 6, the maxima of the transforms are much more accurate.

(a) (b) (c) (d)
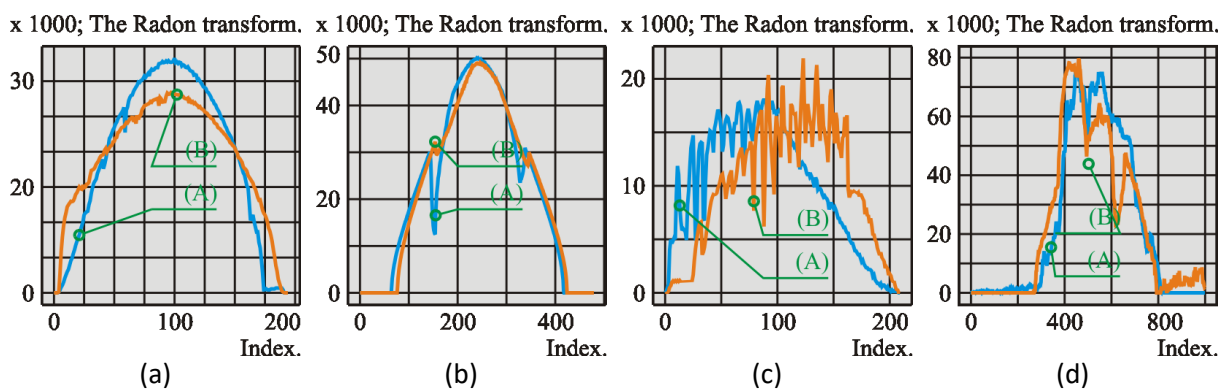
Fig. 8. Estimations for the images in Figures 7. Curves (A): The Radon transforms on the X-axis. Curves (B): The Radon transforms on the Y-axis

The implementation of the forgetting factor improved the accuracy of the mass-centre estimate especially for the images affected by higher values of noise such as Figures 7, (c) and (d). The implementation of the forgetting factor didn't significantly improve the estimations of the directions of the axes of symmetry, Table 2.

Table 2. Filtered images. Estimations of the geometrical parameters

Figure / Image label	Figure 7	(a)	(b)	(c)	(d)
Coordinates of the mass centre	X_0	100	239	88	458
	Y_0	97	246	123	460
Angle of major axis	θ	-60	-55	50	50
Angle between major and minor axis	γ	-95	-100	95	95
Ratio between major and minor axis length	β/α	0.656	0.65	0.381	0.672
Image size	N/N	195/195	480/480	210/210	1000/1000

5. Conclusions

In this work, an implementation of the Radon transformation for estimating the coordinates of the mass-centre and the directions of the main axes of symmetry of image objects is presented. The proposed method may be interpreted as a generalization of the implementation of the Radon transformation method for the estimation of the direction of lines within an image. Within this work, we introduced the function of maximum Radon transform, which is a useful tool to estimate the direction of the major axes of symmetry of the image-objects. We also implemented a forgetting-factor-type filter that allowed improving the mass-centre coordinates estimations. The implementation of the proposed method to four classes of different noised image-objects proved to be straightforward and resilient to blur and margin discontinuities. These characteristics recommend this method especially for the embedded and real-time applications.

References

1. Anton L., Pican S. (2001): *Reconstruction and Recognition of the Radar Target Image*. 5th International Conference on Telecommunications in Modern Satellite, Cable and Broadcasting Service (TELSIKS 2001), ISBN 0-7803-7228-X, p. 61-64, https://ieeexplore.ieee.org/document/954849
2. Zhou C., Yang J., Zhao C., Hua G. (2017): *Fast, Accurate Thin-Structure Obstacle Detection for Autonomous Mobile Robots*. 2017 IEEE Conference on Computer Vision and Pattern Recognition Workshops (CVPRW), eISSN: 2160-7516, p. 318-327, https://ieeexplore.ieee.org/document/8014779
3. Franzius M., Dunn M., Einecke N., Dirnberger R. (2017): *Embedded Robust Visual Obstacle Detection on Autonomous Lawn Mowers*. 2017 IEEE Conference on Computer Vision and Pattern Recognition Workshops (CVPRW), eISSN: 2160-7516, p. 361-369, https://ieeexplore.ieee.org/document/8014784
4. Gouillard E.: *Scikit-image: image processing.* http://www.scipy-lectures.org/packages/scikit-image/
5. Kohler T. (2004): *A projection access scheme for iterative reconstruction based on the golden section*. IEEE Symposium Conference Record Nuclear Science 2004, ISSN: 1082-3654, Vol. 6, p. 3961-3965, https://ieeexplore.ieee.org/stamp/stamp.jsp?arnumber=1466745
6. Hejazi M.R., Shevlyakov G., Ho Y-s (2006): *Modified Discrete Radon Transforms and Their Application to Rotation-Invariant Image Analysis*. 2006 IEEE Workshop on Multimedia Signal Processing, p. 429-434, https://ieeexplore.ieee.org/document/4064595
7. Rizzini D.L. (2018): *Angular Radon spectrum for rotation estimation*. Pattern Recognition, ISSN 0031-3203, Vol. 84, p. 182-196, https://doi.org/10.1016/j.patcog.2018.07.017
8. Soderstrom T.S., Stoica P.G. (2004): *System Identification*. Prentice Hall, ISBN 9780138812362, p. 320-324
9. Liang Z.-P., and Lauterbur P.C. (1999): *Principles of Magnetic Resonance Imaging: A Signal Processing Perspective*. IEEE Engineering in Medicine and Biology Society, ISBN: 978-0-780-34723-6, p. 36-44, 187-188